USING HYPERSPECTRAL IMAGERY TO ASSIST FEDERAL FOREST MONITORING AND RESTORATION PROJECTS IN THE SOUTHERN ROCKY MOUNTAINS, COLORADO

BY

Kyle Wamser

Submitted to the graduate degree program in Department of Geography and the Faculty of the Graduate School of the University of Kansas in partial fulfillment of the requirements for the degree of Master of Arts.

Committee members

_____
Stephen Egbert, Chairperson

_____
Terry Slocum

_____
Xingong Li

Date defended: December 19, 2012

The Thesis Committee for W. Kyle Wamser

certifies that this is the approved version of the following thesis:

USING HYPERSPECTRAL IMAGERY TO ASSIST FEDERAL FOREST MONITORING AND RESTORATION PROJECTS IN THE SOUTHERN ROCKY MOUNTAINS, COLORADO

_____

Chairperson: Stephen Egbert

Date approved: December 19, 2012

Abstract

Kyle Wamser

Department of Geography, December 2012

University of Kansas

Hyperspectral imagery and the corresponding ability to conduct analysis below the pixel level have tremendous potential to aid in landcover monitoring. During large ecosystem restoration projects, being able to monitor specific aspects of the recovery over large and often inaccessible areas under constrained finances are major challenges. The Civil Air Patrol's Airborne Real-time Cueing Hyperspectral Enhanced Reconnaissance (ARCHER) can provide hyperspectral data in most parts of the United States at relatively low cost. Although designed specifically for use in locating downed aircraft, the imagery holds the potential to identify specific aspects of landcover at far greater fidelity than traditional multispectral means.

The goals of this research were to improve the use of ARCHER hyperspectral imagery to classify sub-canopy and open-area vegetation in coniferous forests located in the Southern Rockies and to determine how much fidelity might be lost from a baseline of 1 meter spatial resolution resampled to 2 and 5 meter pixel size to simulate higher altitude collection. Based on analysis

comparing linear spectral unmixing with a traditional supervised classification, the linear spectral unmixing proved to be statistically superior. More importantly, however, linear spectral unmixing provided additional sub-pixel information that was unavailable using other techniques. The second goal of determining fidelity loss based on spatial resolution was more difficult to determine due to how the data are represented. Furthermore,the 2 and 5 meter imagery were obtained by resampling the 1 meter imagery and therefore may not be representative of the quality of actual 2 or 5 meter imagery. Ultimately, the information derived from this research may be useful in better utilizing hyperspectral imagery to conduct forest monitoring and assessment.

For everyone at the University of Kansas and in the United States Air Force who helped me work around two years of flying training and two deployments to see this project to completion

Acknowledgements

First, I would like to acknowledge all the help I received from Ms. Carol Mladinich and the United States Geological Survey for providing the data that were used for this project. The USGS is doing amazing work throughout the country using hyperspectral imagery and I am grateful that Carol and her team were willing to allow me access to data that, at the time I received them, were associated with unpublished research.

I would like to thank the members of the Geography Department at the University of Kansas for all the assistance working through multiple challenges over several years: Specifically Bev Morey, Bev Koerner and Mel Kroeger. From being readmitted to Graduate School to accessing ArcGIS toolboxes, I would have never been able to finish my thesis without support from all of you.

I also owe a debt of gratitude to all the members of my thesis committee. First, to Professor Xingong Li for being willing to sit on the committee on extremely short notice and after not having worked with me in over four years. Second, to Professor Terry Slocum for not only being on the committee but also playing an instrumental role in coordinating with the Graduate School on multiple challenges I faced. From dual enrollment as an undergraduate in 2007 to reenrollment in 2012, I would never have been able to complete my degree

without Terry's help. Finally, to Professor Steve Egbert for single-handedly helping me get my thesis back on track while I was in Afghanistan and taking over as the committee chair. I truly appreciate all the help and understanding.

Table of Contents

List of Figures

List of Tables

Chapter 1

Introduction

Montane forests throughout the Western United States are currently severely degraded. The environmental conditions are so poor that they "virtually guarantee an onset of serious forest health problems which may lead to large wildfires, reburning, erosion and loss of habitat and property" (Sampson *et al*., 1994). From the Rockies to the Sierras, forest ecosystems are being destroyed by erosion, diseases, fire and insect invasion. The primary reason that these forests are vulnerable to such a diverse range of problems is anthropogenic fire suppression during the past century. When comparing historical reports from the beginning of non-native exploration and settlement to the present, tree densities have increased to at least five times greater in numerous study areas (Covington and Moore, 1994).

One of the principal risks of increased tree densities is greater fire danger to both natural ecosystems and property. Although fire is a critical element of forest regeneration in the Western United States, over 100 years of fuel accumulation in many areas has completely altered the natural burn cycle. Research from California's Klamath Mountains indicates that fire frequencies

have decreased by a factor of 10 in some locations (Taylor and Skinner, 2003). As a result, the fire dynamics often shift from small, regenerating ground fires to massive crown fires with the potential to completely destroy ecosystems that have existed for centuries. Since only three percent of fires account for 95% of land burned, the increase of area lost to fires in the United States from 1.85 million hectares during the 1960s to over 2.5 million hectares from 2000 to 2007 indicates that crown fires in the Western forests account for the vast majority of this rise (National Interagency Fire Center, 2008).

Federal and state forest managers currently face a paradox: fires are necessary to restore ecosystems, but as a result of the prolonged no-burn policies, creating low intensity blazes that stay on the ground is difficult. This problem manifested itself in 2000 when the National Park Service lost containment of a controlled burn near Los Alamos, New Mexico. This blaze destroyed approximately 17,500 hectares and caused one billion dollars in damage but did allow for substantial remote sensing and change analysis of the area (Brumby *et al*., 2001; Karter, 2001). Originally implemented as part of a plan to reduce fire danger near Bandelier National Monument, the result of the efforts was the massive Cerro Grande fire that destroyed over 400 homes. Since this incident, forest managers at all levels of government have struggled to develop techniques that will reduce tree density without the risk of inadvertently setting

uncontrollable wildfires. What is clear is that any restoration program must first reduce fuel loads before controlled burns are conducted.

The Bureau of Land Management (BLM), in conjunction with University of Kansas geographers, is in the process of implementing a forest thinning program that involves the mechanized removal of small to medium sized trees coupled with limited controlled burns during the winter (Whitworth and Reed, 2007). Superficially, this treatment method seems counterintuitive in that it is designed to restore forest ecosystems to a more natural state through the use of heavy equipment as well as burning at times of the year fires would never occur in nature. A critical factor to consider, however, is that most of the Western forests in the U.S. do not exist in a pre-European settlement condition, so damage resulting from even nonhuman sources like lightening will be greatly increased by up to 100 years of fuel accumulation as a result of forest management policy.

Currently, this new technique of forest restoration (mechanical removal and small controlled burns in winter) is being applied in a trial program in several areas in Colorado. Monitoring the forest restoration treatments is a critical aspect of ensuring success and avoiding potentially adverse effects. Whenever an environment is disturbed, it is put under a certain amount of stress that often alters biological processes. The goal of the restoration treatment is to cause a shift from closed-canopy forests to more open areas with substantial herbaceous understory

cover as was described in the writings of early European settlers and as revealed in proxy data such as pollen stored in peat and lake bottom sediments. By monitoring these tree-thinned sites, BLM officials will be able to identify and address potential invasive species or prescribe additional treatments should they be deemed necessary. In order to study the effectiveness of the program, extensive field measurements are being recorded at random locations within the treatment zones both before and after the thinning takes place. The ground surveys are capable of providing extremely detailed data on numerous ecological characteristics ranging from soil conditions to animal presence based on scat. The primary drawbacks with these field studies are that they are labor-intensive and time consuming. On a good day, a team of five to eight individuals will likely be able to survey only three sites.

Although certainly not a replacement for field work, high spatial resolution hyperspectral remotely sensed imagery may be useful as a forest monitoring method as the program moves beyond the trial area into a more geographically extended area. Since various levels of thinning are needed throughout tens of millions of hectares managed by government agencies faced with continually tightening budgets, it will be impossible to monitor progress by truck and on foot. Also, some areas under Federal or State management may be essentially inaccessible due to some of the most rugged terrain in the

conterminous United States and the costs and risks of sending teams to these areas.

Researchers with the United States Geological Survey are currently using hyperspectral data obtained from the Civil Air Patrol's Airborne Real-time Cueing Hyperspectral Enhanced Reconnaissance (ARCHER) system to track forest health in Colorado with a focus on pine beetle infestation of coniferous trees (predominately lodgepole pine) and the creation of fire fuels as a result (Cole *et al*., 2009). They have produced multiple generalized classification maps highlighting the added detail of hyperspectral imagery. Also, detection of change over time is a proven capability of remotely sensed data and is being implemented by the USGS to assist with forest health monitoring and fire hazard management.

Substantial progress has been made in producing these landcover classification maps based on hyperspectral imagery and specifically in determining condition of lodgepole pines groves as discussed above (Figure 12). It is not clear, however, if the same imagery would be useful in identifying much finer vegetation types below the single pixel level. Furthermore, it is also unknown how much useful data may be extracted when the reflectance of the vegetation in question is partially blocked by the forest canopy overhead.

The goal of this thesis is to determine if a landcover classification map derived from a pixel purity index is able to provide any additional detail on

undergrowth vegetation when compared to a more traditional supervised classification method. As opposed to a supervised classification where every pixel must fall into a specific landcover category, pixel purity index mapping followed by endmember selection allows for the proportional abundance of each landcover class to be calculated for every pixel. I also will conduct tests to determine the optimum pixel size for classification of smaller vegetation life forms, specifically surface growth including bushes and grass, from airborne hyperspectral imagery and then evaluate the usefulness of supplementing the *insitu* observations with data collected by airborne remote sensing.

Research Background and Relevant Literature

Remote observation of ecosystem dynamics, particularly in deciduous forests, is a longstanding application of remote sensing (Ranson *et al*, 1988). As sensors and processing capabilities improved, scientists were able to more thoroughly analyze less spectrally distinct features such as coniferous growth. Finer features like bushes and grass also became easier to study. The fires that devastated much of Yellowstone National Park in 1988 provided an excellent opportunity to use these improved capabilities study successional vegetation, particularly new-growth needle leaf forests (Knight and Wallace, 1989).

Extensive research conducted in the Greater Yellowstone Area (Yellowstone and Grand Teton National Parks and surrounding National Forests) developed and improved capability to accurately model coniferous forests dominated by a single species (in this case, *Pinus contortus*) using Landsat Thematic Mapper imagery (Blodgett *et al*., 1998; Jakubauskas, 1994, 1996; Jakubauskas and Price, 1993, 1994, 1997, 1998). Additional studies in the same area in 1999 demonstrated added modeling capabilities through the use of geostatistical analysis of the same lodgepole pine forests (Blodgett *et al.*, 2000).

Despite these major improvements in vegetation study based on remotely sensed data, difficulties in identifying plant growth at scales larger than the forest-level persisted into the 2lst century. Specifically, problems differentiating spectrally similar, but biologically distinct pine species were encountered (van Aardt 2000; Gong and Yu, 1997). Additional development in hyperspectral sensors allowed for the production of more detailed vegetation classification maps, with studies indicating that similar species of pine trees grown commercially in the southern United States may be identified as being distinct from one another (van Aardt and Wynne, 2007). Besides using hyperspectral imagery to study uniformly distributed trees grown commercially in the Southeast, researchers have found it to be useful in identifying specific bare soils, which was demonstrated after the Cerro Grande Fire in New Mexico (Kokaly *et al*., 2007). Although this does not necessarily correlate to the resolution (both

spatial and spectral) needed to identify individual herbaceous species, it is clear the technology available is much more capable than in the past and is improving rapidly.

Documentation of forest restoration considerations from a field perspective is much more extensive. Some of the most significant work comes from Northern Arizona and includes publications from as far back as the mid-1980s (Covington and Sackett, 1986). The group of scientists from Northern Arizona University initially began by noting the changing fire regimes that were a result of European settlement of the Southwest (Covington and Moore, 1994; Fule *et al*., 1997) and then later moved on to pioneer restoration theory (Covington *et al.*, 2001; Fule *et al*., 2002). Researchers from Flagstaff are still pursuing research in these areas and are currently analyzing the effectiveness of their treatments on a wide array of different ecosystem elements, such as birds (Wightman and Germaine, 2006). Although Northern Arizona has clearly been in the lead in terms of Western forest restoration research for the past two decades, other authors have also added valuable information to the discourse. One group of scientists worked with ponderosa pine restoration in the Four Corners area (Allen *et al*., 2002) while a second group out of the University of Colorado at Boulder worked with a similar ecosystem in the Front Range west of Denver (Baker *et al*., 2007). Other smaller groups of scientists from Montana and the University of Arizona considered similar problems, with the consensus being that forest

restoration was necessary to prevent catastrophic wildfires. Many of the restoration techniques that were proposed do not differ greatly from what is currently being applied by various governmental agencies in Colorado.

The most relevant research publications related to forest monitoring and restoration come from the USGS in Colorado. Researchers are currently in the process of developing techniques using high spatial resolution hyperspectral data to determine the level and extent of pine beetle damage to coniferous trees (Cole *et al*., 2009). Due to their focus on determining the condition of coniferous groves, they have chosen to classify all other vegetation as "deciduous/grassland." This leaves open the question of the utility of hyperspectral imagery in accurately classifying the smaller vegetation both in the open and under a forest canopy at finer levels of detail.

Chapter 2: Improving Landcover Classification of Non-coniferous Vegetation in Grand County, Colorado Through Linear Spectral Unmixing

Statement of Hypothesis and Research Goals

The goal of this research is to explore the value of using linear spectral unmixing of Airborne Real-time Cueing Hyperspectral Enhanced Reconnaissance (ARCHER) hyperspectral imagery to classify sub-canopy and open area vegetation in forests located in the Southern Rockies. In order to address this goal, the following null hypothesis was addressed:

Null Hypothesis *- There is no significant difference between the classifications of non-coniferous vegetation derived from linear spectral unmixing and a supervised classification at the pixel level within the study area.*

This hypothesis addresses how to improve the use of hyperspectral imagery for mapping non-coniferous vegetation in the study environment and whether sub-pixel methodologies provide superior results when compared to more traditional landcover classification analysis. This analysis will be done at the full 1-meter spatial resolution of the ARCHER imagery in order to obtain the most

refined results. The primary goal will be to determine if the linear spectral unmixing approach to determine the percent composition of a particular type of vegetation in each pixel is superior to a supervised classification performed on classes taken from a minimum noise fraction transformation. If this null hypothesis is rejected it means that a more realistic estimate of landcover was made at the sub-pixel level using linear spectral unmixing or the more conventional supervised classification was statistically superior. If not rejected, no significant difference was observed between either method.

The accuracy assessment will rely primarily on root-mean-square (RMS) error computation and ground verification information derived from high resolution imagery of the area that was withheld from the model design for this specific purpose. The RMS error is found by comparing each individual pixel to either endmembers or data from a spectral library. The lower the RMS error, the better the spectral match. Besides assessing the model mathematically, visual analysis will also be conducted. Although not ground truth points in the literal sense, the panchromatically sharpened images at 0.20-meter spatial resolution available in both true color and color infrared are considered to be sufficient in determining relatively broad landcover classes in the study environment. Furthermore, the data from the panchromatic camera and hyperspectral imager are acquired simultaneously. In many cases, obtaining ground truth points at the same time as the imagery may be cost prohibitive. Collecting ground measurements at a

different time could also introduce additional error. The withholding of the high-resolution imagery for accuracy assessment as was done during this research may be a good compromise depending on the specific study goals.

Study Area

The study area is centered on a location approximately 10 miles south of Granby, Colorado in the vicinity of 39° 57' N, 105° 58' W. The elevation range is 2000 feet, with low points in valleys down to 8,500 feet and hilltops at 10,500 feet. The majority of the area lies within the Arapahoe National Forest and there are few permanent man-made structures. Logging roads are the primary anthropogenic feature on the landscape and they are present in substantial numbers throughout the research site. A single large set of power lines traverses the study area running east to west. A few trucks and recreational vehicles are visible in the imagery but they do not appear to be permanent features. Several rock outcroppings also occur throughout the area. The final prominent non-vegetation surface features are several anthropogenic clear cuts of varying age. After detailed study of the panchromatically sharpened images, the most recent appear to be associated with the removal of large numbers of dead trees in stands likely suffering from pine beetle infestation. Hydrological features are limited to small streams with earthen dams creating small ponds in the valleys. Several low-

lying areas also present evidence that indicates seasonal water flow, likely a result of both spring snow melt and flash flooding in the summer.

Vegetation features may be divided into three broad categories: dense forest, anthropogenically thinned forest, and grasslands/low vegetation. The dense forest areas appear to be unhealthy based on imagery analysis, as a large portion of the trees are dead or under stress. This is supported by multiple US Government reports and research studies conducted in the region (Cole *et al*., 2009; Collins *et al*., 2010). Tree damage caused by a pine beetle infestations is readily apparent in the forested areas and is easily recognizable on true color aerial photography. The thinned forests appear generally in better health than the denser groves due to sick or dead trees being intentionally removed. Analysis, particularly in the near infrared, however, shows that even in the thinned areas many trees are still under substantial stress when compared with examples from spectral response libraries. Large areas of grassland and low vegetation areas are primarily located in valleys along the associated hydrological features. Some of this type of vegetation may also be observed below the forested areas and in the clear cuts, but these examples are far less prominent than those seen alongside streams.

All of the imagery was collected on August 25, 2010 at around 1630 Zulu or 1030 Mountain Daylight Time. According to the United States Naval Observatory's astronomical almanac, the sun angle was approximately 53.7° with

an azimuth of 137.6° east of north. Historical weather records show that visibility at Granby, CO at the time of the flight was 9.3 miles with an average wind speed 3.45 mph. The high visibility indicated that aerosols or other airborne particulates were not likely present in large amounts at the time. Relative humidity was between 60 and 65% but this does not necessarily indicate substantial potential water vapor interference since the daily high temperature is only 66.2° F and the atmosphere is thinner at the elevation of the study area (Figure 1).

Methods

For this research, Airborne Real-time Cueing Hyperspectral Enhanced Reconnaissance (ARCHER) imagery of a lodgepole pine dominated forest in Grand County, Colorado was used. The data were provided by the United States Geological Survey (USGS), which originally had the imagery flown in order study forest health conditions during an ongoing pine beetle infestation. The ARCHER system is flown and maintained by the Civil Air Patrol (CAP). The system is fielded on 16 Gippsland GA8 aircraft throughout the United States. Typical missions are flown at 2500 feet above ground level (AGL) and a groundspeed of 100 knots. The system incorporates two sensors: a hyperspectral imager and a high resolution panchromatic camera. The hyperspectral imager is a pushbroom type sensor and incorporates 52 spectral bands ranging from 500 nm

to 1100 nm each with a spectral bandwidth of 11.5 nm. In order to better visualize these bands, a data cube was used to highlight some features of the imagery (Figure 2). The signal to noise ratio under standard conditions is 100:1 and the spatial resolution of the hyperspectral imagery on a typical sortie is one meter. The spatial resolution of the panchromatic imager is eight cm at the standard mission altitude of 2500 feet AGL (ARCHER Technical Specifications, 2005).

Since a primary use of the ARCHER system is for emergency response (detecting chemical spills, finding downed aircraft), many preprocessing tasks are carried out in real time as the data are recorded. Computer algorithms use a combination of global positioning and inertial navigation to automatically geo-reference the data. The onboard system is also capable of showing waterfall displays (real-time moving maps providing imagery of the sensor's current target) that accurately portray what is on the ground. Additionally, the tasks of anomaly detection and spectral response comparison with a database may be accomplished inflight (ARCHER Operations Manual, 2005). These capabilities imply additional corrections that are done by the software (such as for atmospheric conditions) but the data are not transformed into absolute spectral radiance units (Eismann *et al*. 2009). Since the software is proprietary it is not clear exactly what processes are being completed in order to directly compare spectral libraries to the collected data in near real time.

During less time-sensitive applications, more extensive post-flight data preparation may be completed on the ground. One tool included with the ARCHER ground station is the GeoSharp program. This software allows for users to automatically combine hyperspectral data with the high resolution imagery in order to create a panchromatically sharpened image. True color and color infrared images for more detailed area study are commonly used, although the user may assign any three spectral bands for visualization. The data provided to the USGS used in this study included the full hyperspectral imagery products, subsets of these data for easier processing, the full panchromatic dataset and finally GeoSharp imagery in true color and several versions of color infrared. All data were geo-registered and processed using the onboard software.

The first step of processing was to extract the data to be analyzed. This was accomplished by mosaicking the four flight lines associated with the study area. This resulted in over eight square kilometers of coverage, of which approximately half was pine forest. All data processing conducted on the imagery relied on the Environment for Visualizing Images (ENVI) software package. This was the most logical choice for data analysis because the data are compiled in an ENVI-based format and the software package included many of the algorithms required to manipulate hyperspectral imagery. Besides hyperspectral analysis capabilities, ENVI also includes standard remote sensing tools including preprocessing functions as well as several methods that are used with more

conventional classification of multispectral data. ArcMap 10 and Google Earth were employed for data visualization as well as map production, while SPSS was used for statistical analysis.

Research presented at the 2010 Association of American Geographers annual meeting (Mladinich and Slonecker, 2010) indicated that all previous applications using ARCHER imagery had relied on uncalibrated data due to the fact that all users of the ARCHER platform to date had relied entirely on the system's ability to detect change within the imagery, but had need to standardize data for outside comparison. In other words, all users of the system accepted the onboard processing of the data as delivered and did not perform any additional radiometric corrections to account for atmospheric conditions or sensor calibration. With hyperspectral imagery, the shape of the spectral response curve is more important than the magnitude of the responses across the spectrum. The ARCHER software used inflight is designed based on this concept and the need for additional corrections on the ground has been limited. After testing four radiometric correction methods, Mladinich and Slonecker (2010) found, based on visual inspection, that the empirical line calibration method appeared to be the most accurate, but with the drawback of requiring ground truthing. In general, the use of spectral library data requires substantial post-processing of the imagery for accurate comparison of response curves. However, this is not necessarily true

with the ARCHER system as it is specifically designed to match observations to known spectra in flight.

Without *in situ* measurements of the study area, the empirical line calibration method recommended by Mladinich and Slonecker (2010) was not a viable option. Two other algorithms that have been recently applied by researchers to make atmospheric corrections to hyperspectral data are the QUick Atmosphic Correction (QUAC) and the Fast Line-of-sight Atmospheric Analysis of Spectral Hypercube (FLAASH) methods. A change detection study conducted by the Air Force Research Laboratory (AFRL) discussed both methods as viable options, with FLAASH being somewhat more difficult to implement due to a requirement of absolute sensor calibration (Eismann *et al*., 2008). The Air Force team chose to address atmospheric interference by standardizing their measurements using the Normalized Difference Vegetation Index (NDVI) and then conducting a linear transformation. Further research conducted in India (Agrawal and Sarup, 2011) found that QUAC and FLAASH performed similarly in terms of accuracy of correction with QUAC being the preferred method for addressing unknown areas. As no results in this study were compared directly to either ground measurements or spectral response library information, no additional specific atmospheric corrections were applied. A certain portion of noise was removed, however, due to the nature of the processing algorithms used in order to develop the final land cover class reflectance models.

Often, the next step of preprocessing hyperspectral data is to conduct geometric corrections. Since the data were already orthorectified using the onboard GPS/INS information as well as a 30-meter Digital Elevation Model (DEM), no further geometric corrections were conducted. It should be noted, however, that with the high spatial resolution of the imagery (around one meter) combined with ground measurements conducted using high accuracy GPS units, current in-flight geometric rectification techniques to ARCHER data may not be adequate for certain applications. This was highlighted in the work conducted by the AFRL while studying change detection of small objects in various environmental settings (Eismann *et al*., 2008). High resolution LiDAR elevation profiles coupled with refined georeferencing may be required in the future if ever smaller levels of change are being studied.

Once the radiometric condition of the imagery was addressed and the data were verified as being properly georegistered by visual comparison to a Grand County parcel map, the next step was to reduce the dimensionality of the imagery through the use of a minimum noise fraction transformation. Reducing data dimensionality is important because of the high collinearity between bands and the large data volume due to extremely high spatial resolution. A minimum noise fraction (MNF) transformation uses cascading principal components analyses (PCA) in order to uncorrelate the data and remove noise (Boardman and Kruse, 1994). The results of the MNF transformation are multiple eigenvectors that are

essentially uncorrelated single layer raster graphics that may be visualized in the same manner as spectral bands. The advantage of reducing the dimensionality of a hyperspectral dataset is that the data are much easier to process because of the reduction in data volume and a reduced number of bands (Zare, 2008). A disadvantage, however, is that hyperspectral data contain information at the sub-pixel level. It is possible that eigenimages that appear to be purely noise when visualizing them actually contain useful data.

In selecting which eigenvectors to use, both a visualization technique and careful study of eigenvalues were employed. This reduced the possibility of discarding data that were relevant to land cover classification. Once completed, eigenimages 1-12 were selected for use in further processing (Figure 3). The graph of eigenvalues was favored slightly over visualization in order to facilitate study at the sub-pixel scale where normal raster image study and map algebra techniques are insufficient for thorough analysis.

Once the appropriate eigenimages had been selected, a supervised classification was conducted based on the USGS study classes and feature identification using both true color and color infrared variations of the hyperspectral imagery. The maximum likelihood classification algorithm was chosen because it is one of the most widely used classification methods and is probability-based (Lo and Yeung, 2002). Also, research using hyperspectral imagery to map mangroves along the Texas Gulf Coast indicated that after

conducting a minimum noise fraction reduction, a maximum likelihood classification approach resulted in the best overall accuracy (Yang *et al*., 2009).

In order to compare classifications to data that have been ground truthed, classes similar to those considered by the USGS were used. The primary differences were that multiple levels of stress on the coniferous trees were not considered; only healthy and unhealthy/dying vegetation and additional classes of undergrowth were included. The final thematic map include six land cover classes: tan for bare ground, light green for grass, orange for unhealthy trees, dark green for healthy trees, blue for water and olive green for brush (Figure 5).

After the appropriate MNF layers were selected and the supervised classification was completed for later comparison, the next step was to compute a pixel purity index (PPI) in order to select endmembers. Once the pixel purity index was calculated, a density slice was used to reclassify the pixels into more useful ranges. This detailed study of the PPI image and statistics was used to determine the pixels with highest spectral purity. These pixels were then chosen as endmember candidates based on a minimum threshold of three and exported as a region of interest.

The next step was to select and classify the potential endmembers identified using the PPI through n-Dimensional visualization. The visualization allows the user to select endmembers that represent a theoretically discrete spectral response which may be indicative of pixels representing a pure sample of

a particular landcover type. Endmembers were identified both through n-Dimensional visualization as well as the automated process included with the ENVI software. N-dimensional visualization is accomplished by displaying multiple MNF bands as a data cloud and then selecting clusters of the purest pixels located at the corners (Boardman, 1993). The automatic approach first identifies the most dissimilar pixels within the image and then through multiple iterations determines endmembers based on the number requested by the user or when pixels begin to fall into multiple categories, whichever occurs first. In order to reduce the variability of manually selecting endmembers, the automatic selection method was applied throughout the research.

With endmembers computed, a model of pixel concentration based on these elements was conducted using linear spectral unmixing. The linear spectral unmixing algorithm uses the class mean data that were derived previously in order to determine fractional abundance. With no thermal bands present, different surface temperatures did not challenge the linearity assumption of the model. The output display of a single land cover class provides a monochromatic image where light values indicate high concentrations of the material class while dark areas indicate a smaller percent composition. Multiple classes may be displayed using the red, green and blue color assignments, but interpretation may be difficult due to the complexity of the representation. The output data are the single band for each endmember-defined class as well as a root mean square

graphic for error analysis. The selected bands represented the same classes of bare ground, grass, unhealthy trees, healthy trees, water, and brush. The non-coniferous vegetation model was then coupled with the RMS error output and reclassified using another maximum likelihood supervised classification into the categories of "grass" and "not grass" (these terms were used in place of "non-coniferous vegetation" due to software title character limitations) for an accuracy assessment.

Results and Discussion

As expected based on the classifications presented by the USGS scientists (Sloan, 2010), a typical analysis at the pixel level does not appear to identify much vegetation below the forest canopy upon visual inspection. In other words, there are few light green shaded pixels representing non-coniferous vegetation found within large areas classified as forest. This is true in both the USGS model extraction (Figure 12) as well as the one developed for this research using a maximum likelihood supervised classification (Figure 5). Since both of these models were created using traditional classification methods, all pixels must be placed into a single category. Even if a substantial amount of non-coniferous vegetation was present below the coniferous vegetation, these models much select

one or the other, not a mixture of both. This initial finding suggests that sub-pixel analysis could indeed be of value.

The only statistic that is useful for analyzing model accuracy below the pixel level is the RMS error (and associated image) calculated during the unmixing process (Foppa *et al*., 2002). By analyzing the RMS error in conjunction with either ground data or detailed imagery, it is possible to determine the specific areas or feature classes that are the most accurate. Based on this concept and noting that lighter shading represents less error, the areas of least difference between the model and the endmember appear to be bare ground. Coniferous tree cover seems to generally have the highest RMS values. Non-coniferous vegetation classification appears to perform fairly well based on the shading image; however, the magnitude of the RMS errors vary somewhat depending on which particular grassy spot is observed (Figure 6). In all cases the RMS error was below 0.01. This value is scale-dependent and is not a direct measurement of absolute error but no landcover class appeared drastically different than another, either with higher or lower RMS error values.

Although further partial pixel validation was not possible without *in situ* data, an accuracy assessment of the model in predicting non-coniferous vegetation per pixel was accomplished by selecting training sites from the panchromatically-sharpened imagery that was previously withheld for the specific purpose of model validation. First, the classification map originally developed using a maximum

likelihood approach was assessed (Table 1). The overall accuracy of the model was 77% with a Kappa Coefficient of 0.71. The producer and user accuracies for the non-coniferous vegetation classification (or "grass" category) were 97% and 88%, respectively.

Next, the ability of the non-coniferous vegetation prediction model derived using linear spectral unmixing was assessed. Compared to the original classification map, this prediction model was indeed more accurate with an overall score of 97%. The Kappa Coefficient was 0.94 with producer accuracy of 100% and 95% user accuracy. As discussed before, these values do not provide any direct information on model performance in the sub-pixel realm, but at the same time it is possible to assert that the model designed specifically to predict non-coniferous vegetation performed successfully.

Chapter 3: Determining Optimum Spatial Resolution of a Non-coniferous Vegetation Model Developed from Hyperspectral Imagery

Statement of Hypothesis and Research Goals

The goal of this research is to explore the optimal spatial resolution of hyperspectral imagery from the Airborne Real-time Cueing Hyperspectral Enhanced Reconnaissance (ARCHER) sensor for a non-coniferous vegetation model based on linear spectral unmixing in the Southern Rockies. In order to accomplish the goal, the following null hypothesis was addressed:

Null Hypothesis *- There is no significant difference in the classifications produced by liner spectral unmixing between 1 meter, 2 meter and 5 meter imagery in classifying non-coniferous vegetation in a lodgepole pine dominated forest within the study area.*

This hypothesis will be useful in determining the best spatial resolution for classifying vegetation in the study environment. Being able to use lower spatial resolution imagery is important when dealing with hyperspectral data. When looking at a single data layer in panchromatic format, 2 meter imagery is

approximately 1/4 the size of 1 meter imagery in terms of memory required for storage and use. Five meter imagery is 1/25 the size of 1 meter imagery. The ARCHER sensor provides users with 52 discrete spectral layers and as such, data size and processing times are major considerations. If the null hypothesis is not rejected, the conclusion may be drawn that substantial amounts of memory and processing time could be saved without a significant reduction in the overall accuracy by employing lower resolution imagery. It also may be possible to cover larger areas in a single overflight by allowing the aircraft to fly higher to acquire lower resolution imagery, thereby saving time and money.

Study Area

The study area is centered on a location approximately 10 miles south of Granby, Colorado in the vicinity of 39° 57' N, 105° 58' W. The elevation range is 2000 feet, with low points in valleys down to 8,500 feet and hilltops at 10,500 feet. The majority of the area lies within the Arapahoe National Forest and there are few permanent man-made structures. Logging roads are the primary anthropogenic feature on the landscape and they are present in substantial numbers throughout the research site. A single large set of power lines traverses the study area running east to west. A few trucks and recreational vehicles are visible in the imagery but they do not appear to be permanent features. Several

rock outcroppings also occur throughout the area. The final prominent non-vegetation surface features are several anthropogenic clear cuts of varying age. After detailed study of the panchromatically sharpened images, the most recent appear to be associated with the removal of large numbers of dead trees in stands likely suffering from pine beetle infestation. Hydrological features are limited to small streams with earthen dams creating small ponds in the valleys. Several low-lying areas also present evidence that indicates seasonal water flow, likely a result of both spring snow melt and flash flooding in the summer.

Vegetation features may be divided into three broad categories: dense forest, anthropogenically thinned forest, and grasslands/low vegetation. The dense forest areas appear to be unhealthy based on imagery analysis, as a large portion of the trees are dead or under stress. This is supported by multiple US Government reports and research studies conducted in the region (Cole *et al*., 2009; Collins *et al*., 2010). Tree damage caused by a pine beetle infestations is readily apparent in the forested areas and is easily recognizable on true color aerial photography. The thinned forests appear generally in better health than the denser groves due to sick or dead trees being intentionally removed. Analysis, particularly in the near infrared, however, shows that even in the thinned areas many trees are still under substantial stress when compared with examples from spectral response libraries. Large areas of grassland and low vegetation areas are primarily located in valleys along the associated hydrological features. Some of

this type of vegetation may also be observed below the forested areas and in the clear cuts, but these examples are far less prominent than those seen alongside streams.

All of the imagery was collected on August 25, 2010 at around 1630 Zulu or 1030 Mountain Daylight Time. According to the United States Naval Observatory's astronomical almanac, the sun angle was approximately 53.7° with an azimuth of 137.6° east of north. Historical weather records show that visibility at Granby, CO at the time of the flight was 9.3 miles with an average wind speed 3.45 mph. The high visibility indicated that aerosols or other airborne particulates were not likely present in large amounts at the time. Relative humidity was between 60 and 65% but this does not necessarily indicate substantial potential water vapor interference since the daily high temperature is only 66.2° F and the atmosphere is thinner at the elevation of the study area (Figure 1).

Methods

For this research, Airborne Real-time Cueing Hyperspectral Enhanced Reconnaissance (ARCHER) imagery of a lodgepole pine dominated forest in Grand County, Colorado was used. The data were provided by the United States Geological Survey (USGS), which originally had the imagery flown in order study forest health conditions during an ongoing pine beetle infestation. The

ARCHER system is flown and maintained by the Civil Air Patrol (CAP). The system is fielded on 16 Gippsland GA8 aircraft throughout the United States. Typical missions are flown at 2500 feet above ground level (AGL) and a groundspeed of 100 knots. The system incorporates two sensors: a hyperspectral imager and a high resolution panchromatic camera. The hyperspectral imager is a pushbroom type sensor and incorporates 52 spectral bands ranging from 500 nm to 1100 nm each with a spectral bandwidth of 11.5 nm. In order to better visualize these bands, a data cube was used to highlight some features of the imagery (Figure 2). The signal to noise ratio under standard conditions is 100:1 and the spatial resolution of the hyperspectral imagery on a typical sortie is one meter. The spatial resolution of the panchromatic imager is eight cm at the standard mission altitude of 2500 feet AGL (ARCHER Technical Specifications, 2005).

Since a primary use of the ARCHER system is for emergency response (detecting chemical spills, finding downed aircraft), many preprocessing tasks are carried out in real time as the data are recorded. Computer algorithms use a combination of global positioning and inertial navigation to automatically geo-reference the data. The onboard system is also capable of showing waterfall displays (real-time moving maps providing imagery of the sensor's current target) that accurately portray what is on the ground. Additionally, the tasks of anomaly detection and spectral response comparison with a database may be accomplished inflight (ARCHER Operations Manual, 2005). These capabilities imply additional

corrections that are done by the software (such as for atmospheric conditions) but the data are not transformed into absolute spectral radiance units (Eismann *et al*. 2009). Since the software is proprietary it is not clear exactly what processes are being completed in order to directly compare spectral libraries to the collected data in near real time.

During less time sensitive applications, more extensive post-flight data preparation may be completed on the ground. One tool included with the ARCHER ground station is the GeoSharp program. This software allows for users to automatically combine hyperspectral data with the high resolution panchromatic imagery in order to create a panchromatically sharpened image. True color and color infrared images for more detailed area study are commonly used, although the user may assign any three spectral bands for visualization. The data provided to the USGS used in this study included the full hyperspectral imagery products, subsets of these data for easier processing, the full panchromatic dataset and finally GeoSharp imagery in true color and several versions of color infrared. All data were geo-registered and processed using the onboard software.

The first step of processing was to extract the data to be analyzed. This was accomplished by mosaicking the four flight lines associated with the study area. This resulted in over eight square kilometers of coverage, of which approximately half was pine forest. All data processing conducted on the imagery

relied on the Environment for Visualizing Images (ENVI) software package. This was the most logical choice for data analysis because the data are compiled in an ENVI-based format and the software package includes many of the algorithms required to analyze hyperspectral imagery. Besides - hyperspectral analysis capabilities, ENVI also includes standard remote sensing tools, includig preprocessing functions, as well as several image processing methods that are used with more conventional classification of multispectral data. ESRI ArcMap 10 and Google Earth were employed for data visualization as well as map production, while SPSS was used for statistical analysis.

Research presented at the 2010 Association of American Geographers annual meeting (Mladinich and Slonecker, 2010) indicated that all previous applications using ARCHER imagery had relied on uncalibrated data due to the fact that all users of the ARCHER platform to date had relied entirely on the system's ability to detect change within the imagery, but had need to standardize data for outside comparison. In other words, all users of the system accepted the onboard processing of the data as delivered and did not perform any additional radiometric corrections to account for atmospheric conditions or sensor calibration. With hyperspectral imagery, the shape of the spectral response curve is more important than the magnitude of the responses across the spectrum. The ARCHER software used inflight is designed based on this concept and the need for additional corrections on the ground has been limited. After testing four

radiometric correction methods, Mladinich and Slonecker (2010) found, based on visual inspection, that the empirical line calibration method appeared to be the most accurate, but with the drawback of requiring ground truthing. In general, the use of spectral library data requires substantial post-processing of the imagery for accurate comparison of response curves. However, this is not necessarily true with the ARCHER system as it is specifically designed to match observations to known spectra in flight.

Without *in situ* measurements of the study area, the empirical line calibration method recommended by Mladinich and Slonecker (2010) was not a viable option. Two other algorithms that have been recently applied by researchers to make atmospheric corrections to hyperspectral data are the QUick Atmosphic Correction (QUAC) and the Fast Line-of-sight Atmospheric Analysis of Spectral Hypercube (FLAASH) methods. A change detection study conducted by the Air Force Research Laboratory (AFRL) discussed both methods as viable options, with FLAASH being somewhat more difficult to implement due to a requirement of absolute sensor calibration (Eismann *et al*., 2008). The Air Force team chose to address atmospheric interference by standardizing their measurements using the Normalized Difference Vegetation Index (NDVI) and then conducting a linear transformation. Further research conducted in India (Agrawal and Sarup, 2011) found that QUAC and FLAASH performed similarly in terms of accuracy of correction with QUAC being the preferred method for

addressing unknown areas. As no results in this study were compared directly to either ground measurements or spectral response library information, no additional specific atmospheric corrections were applied. A certain portion of noise was removed, however, due to the nature of the processing algorithms used in order to develop the final land cover class reflectance models.

Often, the next step of preprocessing hyperspectral data is to conduct geometric corrections. Since the data were already orthorectified using the onboard GPS/INS information as well as a 30-meter Digital Elevation Model (DEM), no further geometric corrections were conducted. It should be noted, however, that with the high spatial resolution of the imagery (around one meter) combined with ground measurements conducted using high accuracy GPS units, current in-flight geometric rectification techniques to ARCHER data may not be adequate for certain applications. This was highlighted in the work conducted by the AFRL while studying change detection of small objects in various environmental settings (Eismann *et al*., 2008). High-resolution LiDAR elevation profiles coupled with refined georeferencing may be required in the future if ever smaller levels of change are being studied.

Once the radiometric condition of the imagery was addressed and the data were verified as being properly georegistered by a visual comparison to a Grand County parcel map, all 52 spectral bands present in the imagery were resampled to two and five meter spatial resolution in order to simulate data collection at a

lower spatial resolution. The next step was to reduce the dimensionality of all three sets of imagery through the use of a minimum noise fraction transformation. Reducing data dimensionality is important because of the high collinearity between bands and the large data volume due to extremely high spatial resolution. A minimum noise fraction (MNF) transformation uses cascading principal components analyses (PCA) in order to uncorrelate the data and remove noise (Boardman and Kruse, 1994). The results of the MNF transformation are multiple eigenvectors that are essentially uncorrelated single layer raster graphics that may be visualized in the same manner as spectral bands. The advantage of reducing the dimensionality of a hyperspectral dataset is that the data are much easier to process because of the reduction in data volume and a reduced number of bands (Zare, 2008). A disadvantage is that hyperspectral data contain information at the sub-pixel level. It is possible that eigenimages that appear to be purely noise when visualizing them actually contain useful data.

In selecting which eigenvectors to use, both a visualization technique and careful study of eigenvalues were employed. This reduced the possibility of discarding data that were relevant to landcover classification. Once completed, eigenimages 1-12 were selected for use in further processing (Figure 3). The graph of eigenvalues was favored slightly over visualization in order to facilitate study at the sub-pixel scale where normal raster image study and map algebra techniques are insufficient for thorough analysis.

After the appropriate MNF layers were selected, the next step was to compute pixel purity indices (PPI) in order to select endmembers. Once calculated, a density slice was used to reclassify the pixels into more useful ranges. This detailed study of the PPI images and statistics was used to determine the pixels with highest spectral purity. These pixels were then chosen as endmember candidates based on a minimum threshold of three and exported as a region of interest. This process was repeated for each sample size.

The next step was to select and classify the potential endmembers identified using the PPI through n-Dimensional visualization. The visualization allows the user to select endmembers that represent a theoretically discrete spectral response which may be indicative of pixels representing a pure sample of a particular landcover type. Endmembers were identified both through n-Dimensional visualization as well as the automated process included with the ENVI software. N-dimensional visualization is accomplished by displaying multiple MNF bands as a data cloud and then selecting clusters of the purest pixels located at the corners (Boardman, 1993). The automatic approach first identifies the most dissimilar pixels within the image and then through multiple iterations determines endmembers based on the number requested by the user or when pixels begin to fall into multiple categories, whichever occurs first. In order to reduce the variability of manually selecting endmembers, the automatic selection method was applied throughout the research.

With endmembers computed, a model of pixel concentration based on these elements was conducted using linear spectral unmixing. The linear spectral unmixing algorithm uses the class mean data that were derived previously in order to determine fractional abundance. With no thermal bands present, different surface temperatures did not challenge the linearity assumption of the model. The output display of a single land cover class provides a monochromatic image where light values indicate high concentrations of the material class while dark areas indicate a smaller percent composition. Multiple classes may be displayed using the red, green and blue color assignments, but interpretation may be difficult due to the complexity of the representation. The data output are the single band for each endmember-defined class as well as a root mean square graphic for error analysis. The selected bands represented the same classes of bare ground, grass, unhealthy trees, healthy trees, water and brush.

Once the data were processed and representative models were derived from linear spectral unmixing, the imagery was loaded into GIS software for additional study and visualization. Finally, the reflectance values were converted to scaled integer values and some basic statistical analysis using the Pearson correlation coefficient to compare the classification of non-coniferous vegetation at the three pixel sizes was conducted.

Results and Discussion

The results of the two and five meter pixel resampling of the linear spectral unmixing-derived non-coniferous model were analyzed both visually and statistically. A visual comparison between the images of the original selected study area demonstrated that although detail is lost, no major changes in the classification of non-coniferous vegetation occurred (Figure 9, Figure 10, Figure 11). These results are also supported statistically by both mathematical change detection analysis and data similarity found by computing the Pearson Correlation Coefficient. Change detection was used to determine how closely the lower spatial resolution imagery compared to the 1 meter standard. For example, a 2 meter pixel could be broken down into four different 1 meter pixels. Using a traditional classification method, all of the four sub-pixels will be a single category (either 0% or 100% proportional abundance). By using linear spectral unmixing, a range of proportional abundance is now available. All four sub-pixels will still have identical values, but will be a value on a scale as opposed to purely binary.

A breakdown of the scaled integers into 11 bands with band six in the center representing no change and the five additional bands on either side representing increases or decreases in 20% increments indicated that (with zero-line no-data removed) 98% of the image changed less than 20% in reflectance

(Table 1). Similar results were also observed with the other comparisons. From one-meter spatial resolution to five-meter resolution, 97% of pixels changed less than 20% while the number was 98% from two-meter to five–meter resolution (Table 2, Table 3). Further indicating that the images did not change significantly with increasing pixel size were Pearson Coefficients all in excess of 0.96 but more importantly, correlation was significant at the two-tailed 0.01 level in every case.

Although the data were found to be highly related both visually and statistically at all the pixel sizes, some other considerations should be taken into account before concluding that data with a lower spatial resolution should be used. The first potential drawback is that the data were resampled to larger pixel sizes as opposed to actually being recorded in this manner. A second is associated with the fact that a larger area may be recorded by flying at a higher altitude, resulting in larger pixel sizes. However, this may induce errors associated with more atmosphere between the sensor and the target. This could be more problematic in areas at lower elevations with higher humidity that would produce greater atmospheric scattering, especially in shorter wavelengths. A final consideration is that the ARCHER platform is designed for specific flight parameters. Even if higher altitudes are allowed by aircraft performance, substantial sensor recalibration may be necessary along with additional preprocessing.

Chapter 4

Conclusions

After studying the results produced using linear spectral unmixing, it is evident that substantially more information may be derived using sub-pixel analysis methods when compared to more traditional maximum likelihood data classification techniques. Not only were the overall user and producer errors lower with linear spectral unmixing, but also information about specific landcover classes is available for each pixel. Although the time required to process the imagery is greatly increased, sub-pixel analysis appears to provide a much better representation of the actual non-coniferous vegetation presence within the study area. These results suggest that in order to best utilize ARCHER hyperspectral imagery for landcover mapping, a sub-pixel technique should be applied in most cases.

The optimization of pixel size is a more challenging subject and will likely depend on application. The results of this study indicated that a change from one-meter to five-meter pixel size saw 97% of the sample change less than 20%. Although this information, coupled with the highly significant correlation coefficients, indicates that much information may be retained at lower spatial

resolutions, these results may be artificial due to resampling. If the five-meter data were obtained directly from the aircraft as opposed to resampling from one meter data, it is not clear that the results would be duplicated. Furthermore, the type of landcover being analyzed as well as remote sensing platforms available will play a major role in determining the appropriate (or available) pixel size. For the purposes of this project, the one-meter spatial resolution imagery performed extremely well but the research did suggest that lower spatial resolution would most likely have been acceptable for this specific study.

Ultimately, this research may be useful in helping various organizations concerned with forest management employ limited financial resources more effectively. In many cases, hyperspectral data and the associated sub-pixel analysis have the ability to provide much more detailed landcover information than was previously available with multispectral imagery. By improving the use of remotely sensed data, concerned parties (both private and public) may be able to adequately monitor ground conditions over a large area. Although not a replacement for direct field measurements, these data when fully utilized may be an acceptable compromise between accuracy and cost for certain applications.

Figures

Figure 1: Location of Research Area - Grand County, Colorado

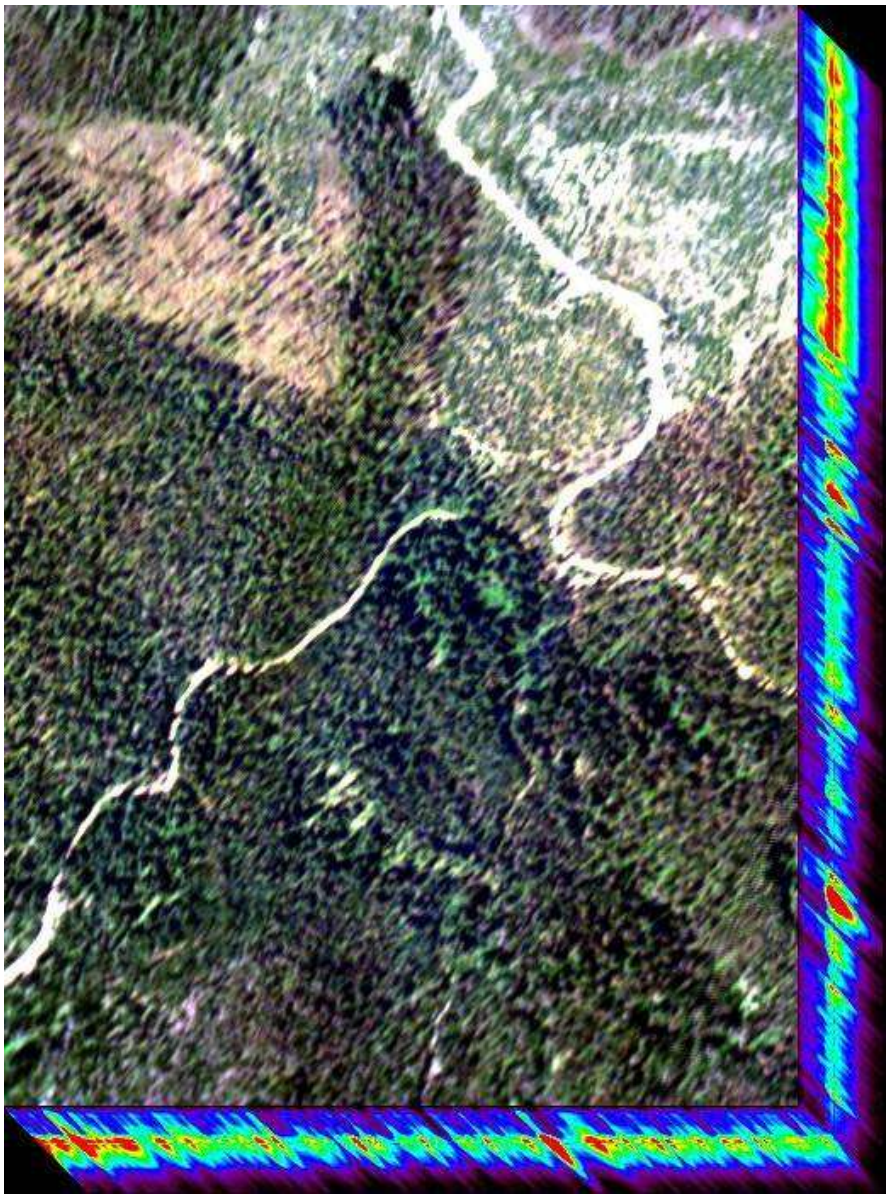

Figure 2: Hyperspectral Data Cube in True Color

The reflectances for each of the 52 bands are indicated by the color ramp below the image on two sides. Although not individually visible, each band is represented by edge shading from violet to red. The edge shading corresponds to the reflectance of the edge pixels. Low reflectance values are displayed as violet with the color ramp increasing to red to display high reflectance. Besides representing the large amount of data, the gradual change from violet to red indicates correlation of nearby bands.

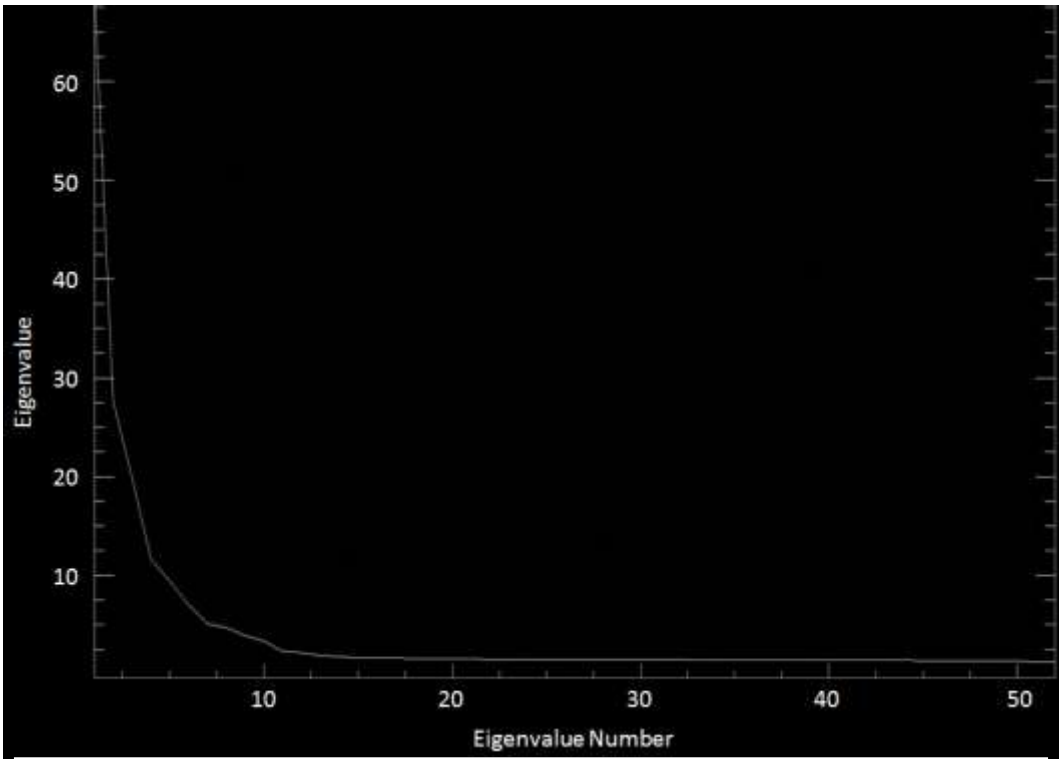

Figure 3: Graph of Eigenvalues by Minimum Noise Fraction Bands

This figure depicts eigenvalues on the y-axis versus the eigenvalue Number (or minimum noise fraction band number) on the x-axis. The eigenvalue is representative of the amount of variance explained by each band. By analyzing this graph along with visualization of the output bands, the 1-12 minimum noise fraction eigenimages were selected and used to create a pixel purity index. Band twelve was the final band selected because it appeared to still explain a small amount of meaningful variance as opposed to pure noise. The number of bands selected is particularly important when conducting pixel purity index mapping as they directly correspond to the number of endmembers available.

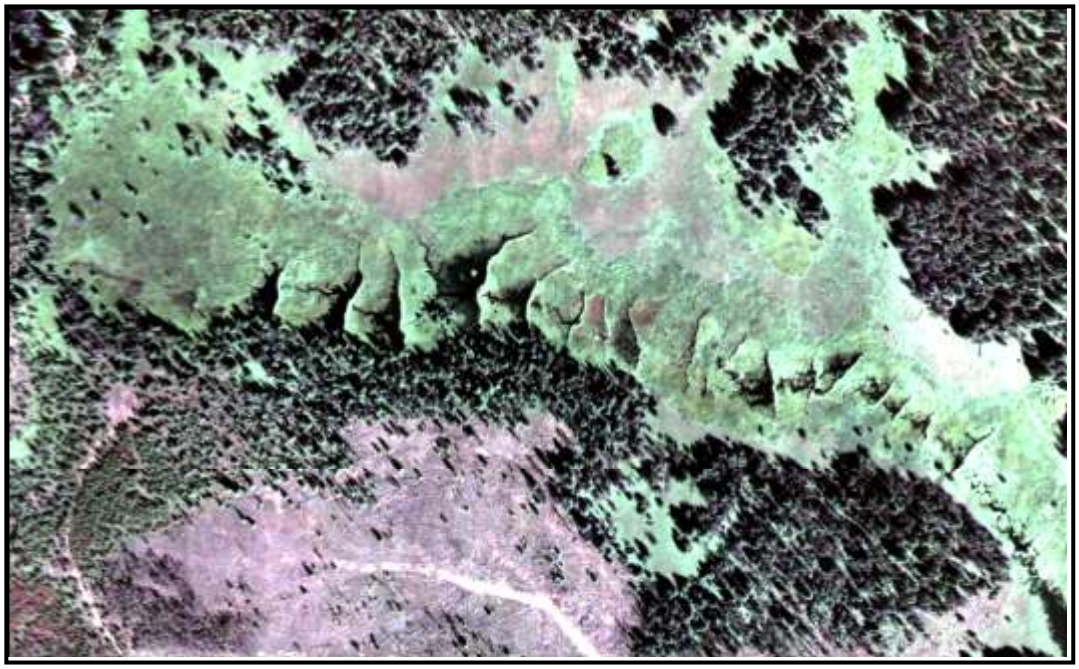

Figure 4: Panchromatically Sharpened Image of Grand County, CO Study Area (650m X 450m)

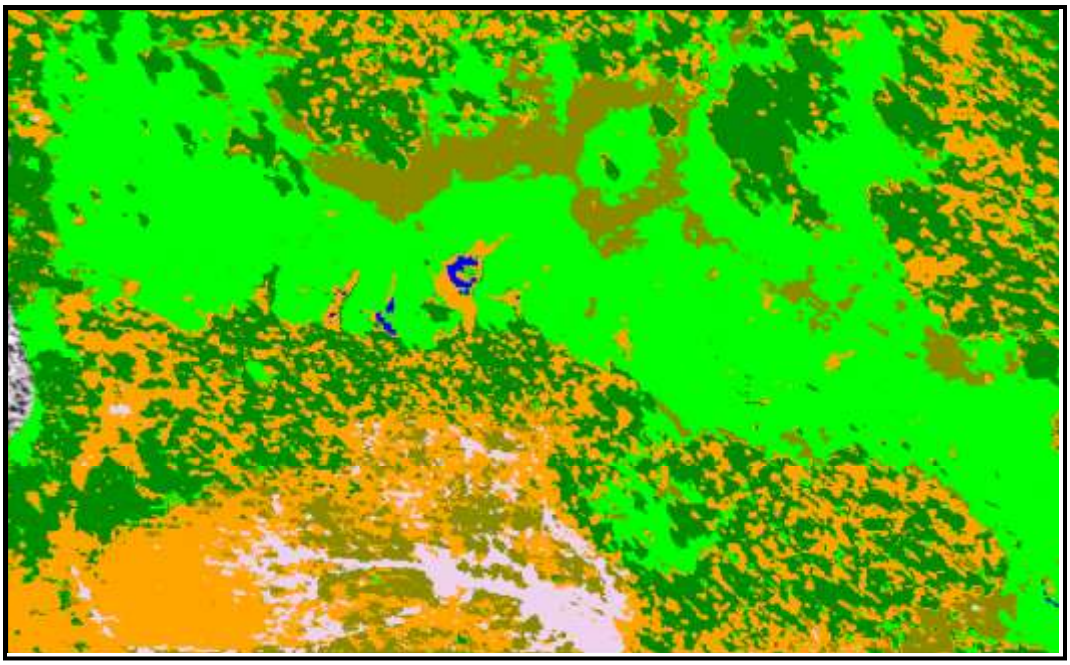

Figure 5: Supervised Classification Map of Extracted Area

Figure 6: Linear Spectral Unmixing RMS Error Image of Extracted Area

The RMS error image represents the only statistical tool that is useful for analyzing model accuracy below the pixel level (Foppa *et al*., 2002). Lower RMS error is represented by the lighter areas and increases as the shade becomes darker. In all case, the RMS error was less than 0.01.

Figure 7: Unmixed Representation of Non-Coniferous Vegetation in Extracted Area

This graphic displays relative abundance of non-coniferous vegetation in the extracted area. Lighter shades indicate high concentrations (by individual pixel) while darker areas represent lower concentrations. The darkest areas in the center are bodies of water with almost no vegetation present.

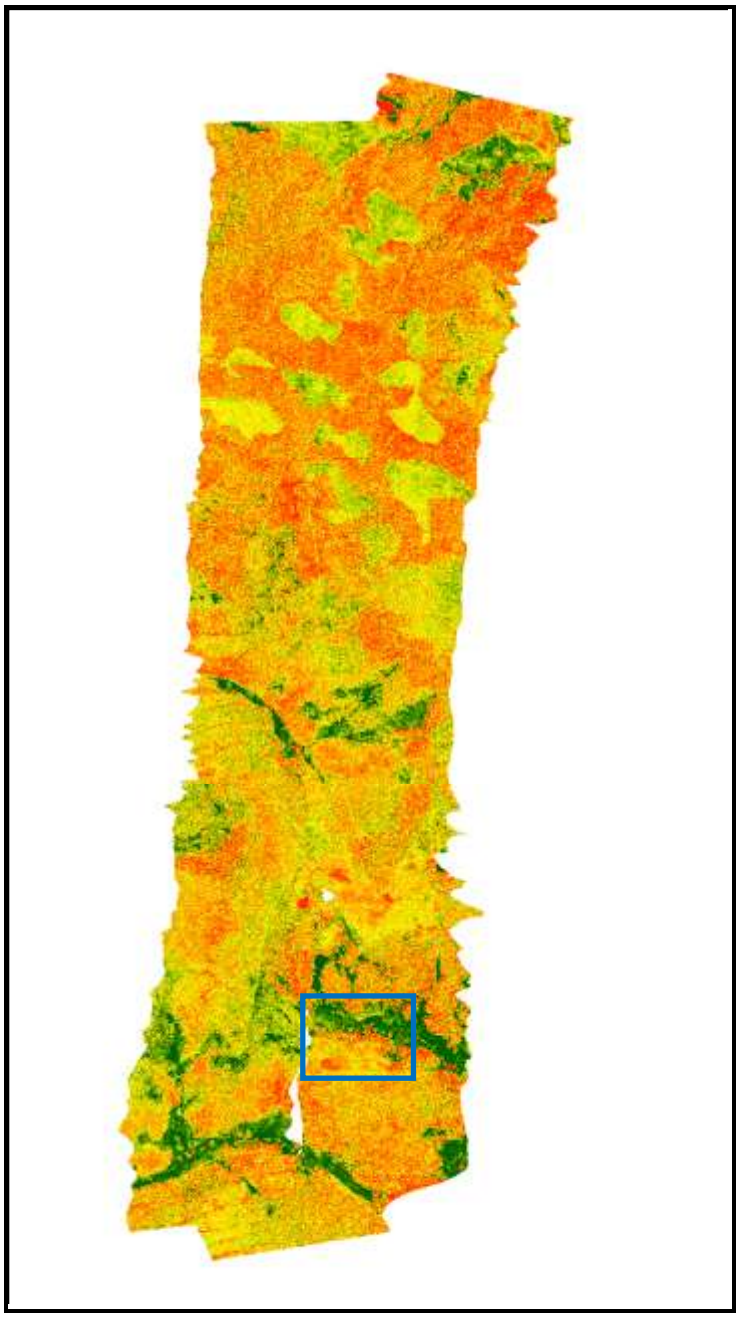

Figure 8: Color Ramp Display of Grass Extraction from Linear Spectral Unmixing at the Full 1 Meter Resolution

The color ramp from green to orange indicates the relative amount of vegetation derived from the grass endmember. High concentrations are represented by green while red indicates low values. The blue rectangle represents the extracted region used in figures 4-7 and 9-11.

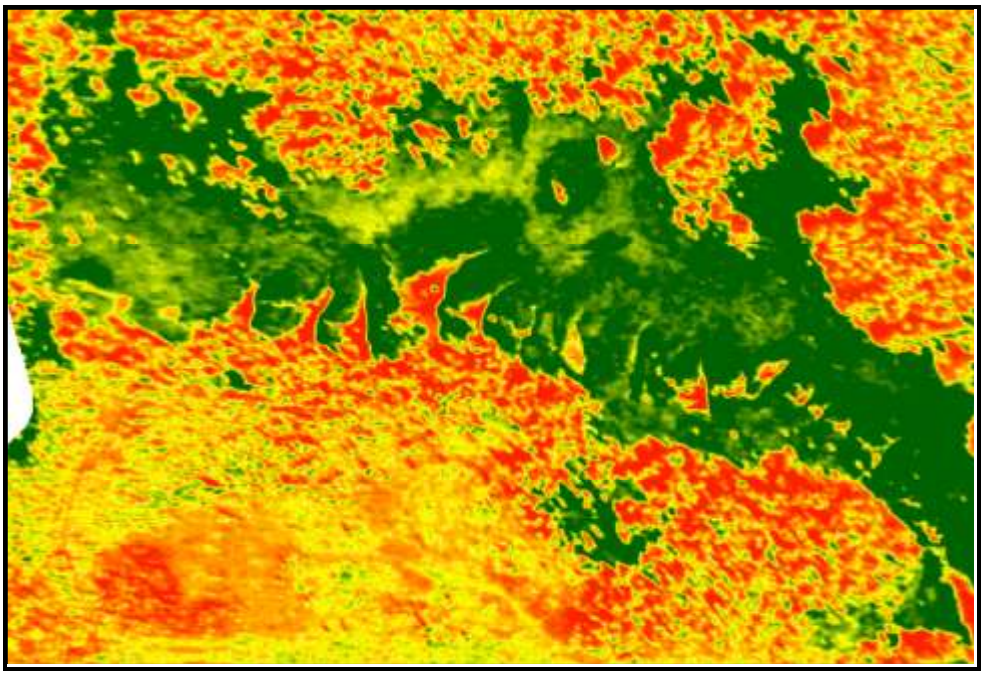

Figure 9: Color Ramp Display of Grass Extraction from Linear Spectral Unmixing, 1 Meter, Extracted Area

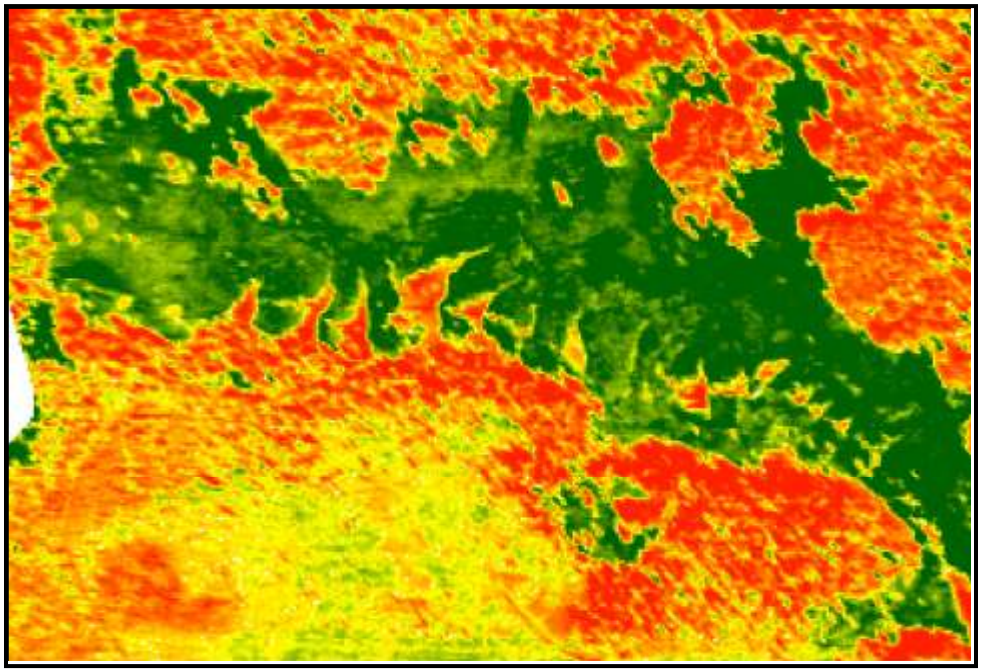

Figure 10: Color Ramp Display of Grass Extraction from Linear Spectral Unmixing, 2 Meter, Extracted Area

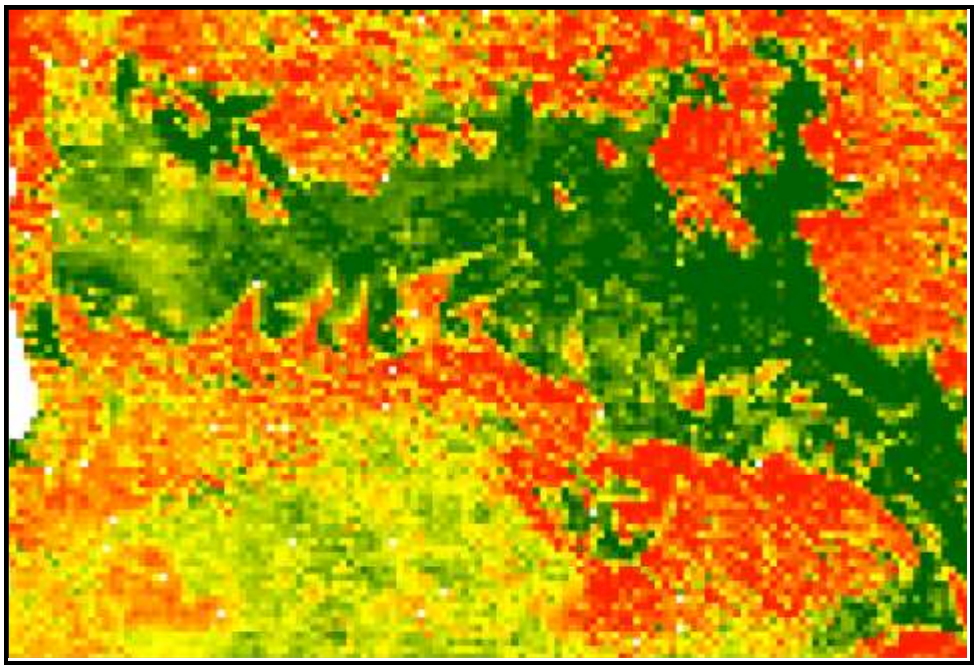

Figure 11: Color Ramp Display of Grass Extraction from Linear Spectral Unmixing, 5 Meter, Extracted Area

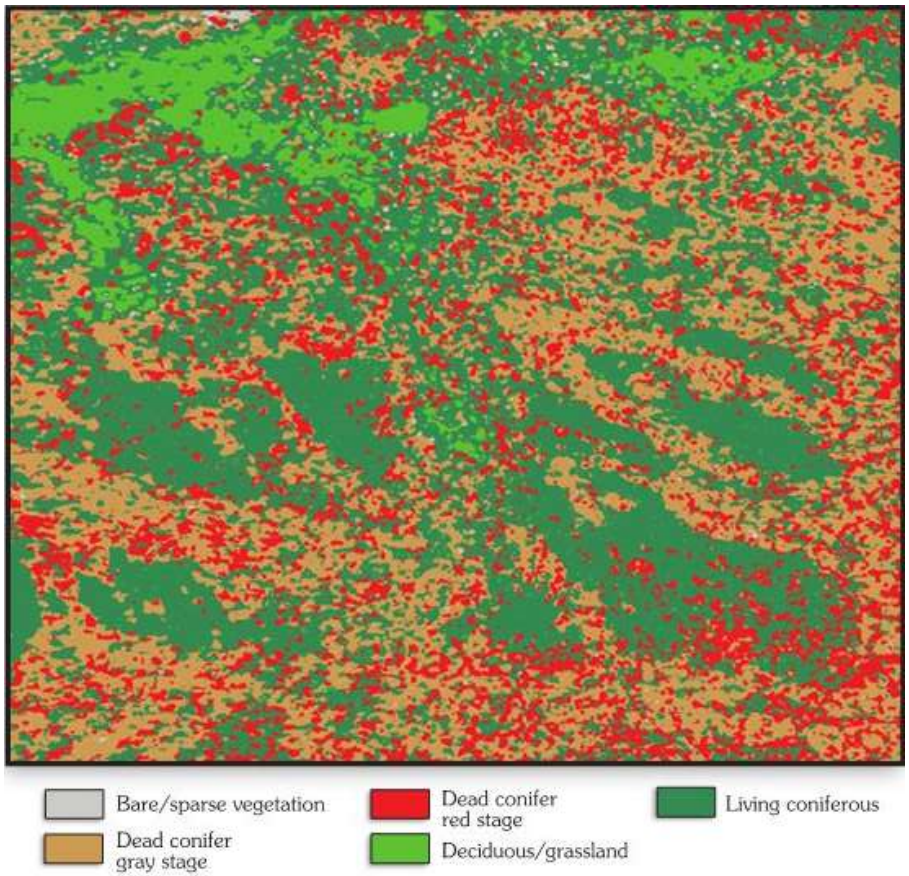

Figure 12: USGS Preliminary Generalized Classification Delineating Multi-Stage Conifer Mortality; from CAP ARCHER Imagery (Sloan, 2010)

Tables

Overall Accuracy = (4134/5356) 77.1845%
Kappa Coefficient = 0.7093

Class	Commission (Percent)	Omission (Percent)	Commission (Pixels)	Omission (Pixels)
Grass [Green]	11.97	2.65	225/1879	45/1699
Bare [Thistle	64.87	41.19	709/1093	269/653
Water [Blue]	0.00	19.81	0/85	21/106
Brush [Yellow	8.32	59.90	43/517	708/1182
Healthy Trees	1.31	23.88	7/533	165/691
Dead Trees [O	19.06	1.37	238/1249	14/1025

Class	Prod. Acc. (Percent)	User Acc. (Percent)	Prod. Acc. (Pixels)	User Acc. (Pixels)
Grass [Green]	97.35	88.03	1654/1699	1654/1879
Bare [Thistle	58.81	35.13	384/653	384/1093
Water [Blue]	80.19	100.00	85/106	85/85
Brush [Yellow	40.10	91.68	474/1182	474/517
Healthy Trees	76.12	98.69	526/691	526/533
Dead Trees [O	98.63	80.94	1011/1025	1011/1249

Table 1: Error Matrix of Original Maximum Likelihood Supervised Classification

Overall Accuracy = (4645/4771) 97.3590%
Kappa Coefficient = 0.9472

Class	Commission (Percent)	Omission (Percent)	Commission (Pixels)	Omission (Pixels)
Grass [Green]	5.10	0.00	126/2471	0/2345
Not Grass [Re	0.00	5.19	0/2300	126/2426

Class	Prod. Acc. (Percent)	User Acc. (Percent)	Prod. Acc. (Pixels)	User Acc. (Pixels)
Grass [Green]	100.00	94.90	2345/2345	2345/2471
Not Grass [Re	94.81	100.00	2300/2426	2300/2300

Table 2: Error Matrix of Maximum Likelihood Supervised Classification on Linear Spectral Unmixing Non-coniferous Vegetation Model

Basic Stats	Min	Max	Mean	Stdev
Band 1	0	11	3.827375	3.174229

Histogram	DN	Npts	Total	Percent	Acc Pct
Band 1	0	5707606	5707606	39.0718	39.0718
	1	22740	5730346	0.1557	39.2275
	2	6623	5736969	0.0453	39.2728
	3	13162	5750131	0.0901	39.3629
	4	39799	5789930	0.2724	39.6353
	5	3116620	8906550	21.3350	60.9704
	6	0	8906550	0.0000	60.9704
	7	5616646	14523196	38.4491	99.4195
	8	40911	14564107	0.2801	99.6995
	9	13617	14577724	0.0932	99.7927
	10	6876	14584600	0.0471	99.8398
	11	23400	14608000	0.1602	100.0000

Table 3: Change Statistics from 1 Meter Resolution to 2 Meter Resolution, Grass Extraction In order to better compare the change between resolutions, the pixel reflectance values were converted into scaled integers and compared against each other. The zero line represents no data while row six shows no change. Each non-zero row above and below row six represents an additional 20 percent of change. In this case, rows five and seven indicate a 20% or less decrease or increase respectively and include 98% of the total points. *Due to the no data on the zero line, all columns other than "number of points" do not provide meaningful information and all values were recalculated with these points excluded. This is also true in Tables 4 and 5.*

Basic Stats	Min	Max	Mean	Stdev
Band 1	0	11	3.876707	3.213265

Histogram	DN	Npts	Total	Percent	Acc Pct
Band 1	0	5689992	5689992	38.9512	38.9512
	1	40368	5730360	0.2763	39.2275
	2	9529	5739889	0.0652	39.2928
	3	19236	5759125	0.1317	39.4245
	4	56287	5815412	0.3853	39.8098
	5	2778733	8594145	19.0220	58.8318
	6	0	8594145	0.0000	58.8318
	7	5880932	14475077	40.2583	99.0901
	8	61293	14536370	0.4196	99.5097
	9	20036	14556406	0.1372	99.6468
	10	9740	14566146	0.0667	99.7135
	11	41854	14608000	0.2865	100.0000

Table 4: Change Statistics from 1 Meter Resolution to 5 Meter Resolution, Grass Extraction

In order to better compare the change between resolutions, the pixel reflectance values were converted into scaled integers and compared against each other. The zero line represents no data while row six shows no change. Each non-zero row above and below row six represents an additional 20 percent of change. In this case, rows five and seven indicate a 20% or less decrease or increase respectively and include 97% of the total points.

Basic Stats	Min	Max	Mean	Stdev	
Band 1	0	11	3.775952	3.139951	
Histogram	DN	Npts	Total	Percent	Acc Pct
Band 1	0	1423359	1423359	38.9748	38.9748
	1	8139	1431498	0.2229	39.1976
	2	2025	1433523	0.0554	39.2531
	3	3910	1437433	0.1071	39.3602
	4	11434	1448867	0.3131	39.6732
	5	881657	2330524	24.1418	63.8150
	6	1	2330525	0.0000	63.8150
	7	1294227	3624752	35.4389	99.2539
	8	12489	3637241	0.3420	99.5959
	9	4000	3641241	0.1095	99.7054
	10	2021	3643262	0.0553	99.7607
	11	8738	3652000	0.2393	100.0000

Table 5: Change Statistics from 2 Meter Resolution to 5 Meter Resolution, Grass Extraction

In order to better compare the change between resolutions, the pixel reflectance values were converted into scaled integers and compared against each other. The zero line represents no data while row six shows no change. Each non-zero row above and below row six represents an additional 20 percent of change. In this case, rows five and seven indicate a 20% or less decrease or increase respectively and include 98% of the total points.

Correlations

		count_1m	count_2m
count_1m	Pearson Correlation	1	.982**
	Sig. (2-tailed)		.000
	N	255	255
count_2m	Pearson Correlation	.982**	1
	Sig. (2-tailed)	.000	
	N	255	255

**. Correlation is significant at the 0.01 level (2-tailed).

Correlations

		count_1m	count_5m
count_1m	Pearson Correlation	1	.964**
	Sig. (2-tailed)		.000
	N	255	255
count_5m	Pearson Correlation	.964**	1
	Sig. (2-tailed)	.000	
	N	255	255

**. Correlation is significant at the 0.01 level (2-tailed).

Correlations

		count_2m	count_5m
count_2m	Pearson Correlation	1	.988**
	Sig. (2-tailed)		.000
	N	255	255
count_5m	Pearson Correlation	.988**	1
	Sig. (2-tailed)	.000	
	N	255	255

**. Correlation is significant at the 0.01 level (2-tailed).

Tables 6 - 8: Pearson Correlation Coefficients between Original and Resampled Pixel Sizes

The Pearson Correlation Coefficient ranges in value from -1 to 1 with positive one describing a relationship perfectly. In all cases, the value of the coefficient is greater than 0.95 and, more importantly, all comparisons are statistically significant at the 0.01 level based on a two-tailed t-test.

Bibliography

Agrawal, G. and J. Sarup. 2011. Comparison of QUAC and FLAASH Atmospheric Correction Modules on EO-1 Hyperion Data of Sanchi. *International Journal of Advanced Engineering Sciences and Technologies.* 4 (1):178-186

Allen, C. D., M. Savage, D. A. Falk, K. F. Suckling, T. W. Swetnam, T. Schulke, P. B. Stacey, P. Morgan, M. Hoffman, and J. T. Klingel. 2002. Ecological Restoration of Southwestern Ponderosa Pine Ecosystems: A Broad Perspective. *Ecological Applications* 12 (5):1418-1433.

ARCHER Technical Specifications. 2005. CAP Advanced Technologies Group. Montgomery, Alabama.

ARCHER Operations Manual. 2005. HSI Technology for the Non-Scientist. Space Computer Corporation.

Baker, W. L., T. T. Veblen, and R. L. Sherriff. 2007. Fire, Fuels and Restoration of Ponderosa Pine-Douglas Fir Forests in the Rocky Mountains, USA. *Journal of Biogeography* 34 (2):251-269.

Blodgett, C., M. E. Jakubauskas, K. Price, and E. Martinko. 2000. Remote Sensing-Based Geostatistical Modeling of Forest Canopy Structure. In ASPRS 2000 Annual Conference, Washington, D.C.

Blodgett, C. B., M. E. Jakubauskas, C. L. Lauver, K. P. Price, and L. Bian. 1998. Geostatistical Modeling of Forest Canopy Structure, Grand Teton National Park. Paper read at Association of American Geographers Annual Meeting at Boston, Massachusetts.

Boardman J. W., 1993. Automating Spectral Unmixing of AVIRIS Data Using Convex Geometry Concepts. Summaries of the 4th Annual JPL Airborne Geosciences Workshop, Jet Propulsion Laboratory, Pasadena, California.

Boardman J. W., and F. A. Kruse, 1994, Automated Spectral Analysis: A Geologic Example using AVIRIS Data, North Grapevine Mountains, Nevada. In Proceedings, Tenth Thematic Conference on Geologic Remote Sensing. Ann Arbor, Michigan.

Brumby, S.P., J. Theiler, S. Perkins, N.R. Harvey, J.J. Szymanski, Genetic Programming Approach to Extracting Features from Remotely Sensed Imagery. Proceedings of the FUSION 2001 at Montreal, Canada.

Cole, C., E. Lile, and J. Briggs. 2009. Hazards Management in Grand County, Colorado—Fire Fuels Characterization. U.S. Geological Survey Fact Sheet. (2009 3078):6.

Collins, B.J., C.C. Rhoads, J. Underhill, and R.M. Hubbard. 2010. Post-harvest Seedling Recruitment Following Mountain Pine Beetle Infestation of Colorado Lodgepole Pine Stands: A Comparison using Historic Survey Records. *Canadian Journal of Forest Research* 40:2452–2456.

Covington, W. W., P. Z. Fule, S. C. Hart, and R. P. Weaver. 2001. Modeling Ecological Restoration Effects on Ponderosa, Pine Forest Structure. *Restoration Ecology* 9 (4):421-431.

Covington, W. W. and M. M. Moore. 1994. Southwestern Ponderosa Forest Structure: Changes since Euro-American Settlement. *Journal of Forestry* 92 (1):39-47.

Covington, W. W., and S. S. Sackett. 1986. Effect of Periodic Burning on Soil-Nitrogen Concentrations in Ponderosa Pine. *Soil Science Society of America Journal* 50 (2):452-457.

Eismann, M. T., J. Meola, A. D. Stocker, S. G. Beaven and A. P. Schaum. 2008. Airborne hyperspectral detection of small changes. *Applied Optics* 47 (28):27-45

Eismann, M. T., A. D. Stocker and N. M. Nasrabadi. 2009. Automated Hyperspectral Cueing for Civilian Search and Rescue. *IEEE Signal Processing* 97 (6): 1031-1055.

Foppa, N. S. Wunderle, and A. Hauser. 2002. Spectral Unmixing of NOAA-AVHRR Data for Snow Cover Estimation. EARSeL eProceedings.

Fule, P. Z., W. W. Covington, and M. M. Moore. 1997. Determining Reference Conditions for Ecosystem Management of Southwestern Ponderosa Pine Forests. *Ecological Applications* 7 (3):895-908.

Fule, P. Z., W. W. Covington, H. B. Smith, J. D. Springer, T. A. Heinlein, K. D. Huisinga, and M. M. Moore. 2002. Comparing Ecological Restoration Alternatives: Grand Canyon, Arizona. *Forest Ecology and Management* 170 (1-3):19-41.

Gong, R. P., and B. Yu. 1997. Conifer Species Recognition: An Exploratory Analysis of *Insitu* Hyperspectral Data. *Remote Sensing of Environment*, 62 (2):189–200

Jakubauskas, M. E., and K. P. Price. 1994. Thematic Mapper Characterization of Coniferous Forest Succession. Paper read at ASPRS-ACSM Annual Meeting, Reno, NV.

Jakubauskas, M. E. 1996. Thematic Mapper Characterization of Lodgepole Pine Seral Stages in Yellowstone National Park, USA. *Remote Sensing of Environment* 56 (2):118-132.

Jakubauskas, M. E. and K. P. Price. 1993. Spectral-Ecological Characterization and Mapping of Forest Cover Types in Yellowstone National Park, Wyoming. Paper read at Second Biennial Scientific Conference on the Greater Yellowstone Ecosystem, at Mammoth, Wyoming.

Jakubauskas, M. E. and K. P. Price. 1997. Empirical Relationships between Structural and Spectral Factors of Yellowstone Lodgepole Pine Forests. *Photogrammetric Engineering and Remote Sensing* 63 (12):1375-1381.

Karter, M. J. 2001. 2000 United States Fire Loss Report. *NFPA Journal* September/October 2001: 82-87.

Knight, D. H. and L. L. Wallace. 1989. The Yellowstone Fires: Issues in Landscape Ecology. *BioScience* 39 (10):700-706.

Kokaly, R. F., B. W. Rockwell, S. L. Haire, and T. V. V. King. 2007. Characterization of Post-Fire Surface Cover, Soils, and Burn Severity at the Cerro Grande Fire, New Mexico, Using Hyperspectral and Multispectral Remote Sensing. *Remote Sensing of Environment* 106 (3):305-325.

Lo, C. P. and A. K. Yeung. 2002. Concepts and Techniques of Geographic Information Systems. Prentice-Hall, Upper Saddle River, New Jersey.

Mladinich, C. S. and E. T. Slonecker. 2010. Calibration of Airborne Real-time Cueing Hyperspectral Enhanced Reconnaissance Imagery. In AAG 2010 Annual Meeting, Washington D.C.

National Interagency Fire Center, 2007 Summary Report. Published online February 2008, retrieved on May 3, 2008.

Ranson, K. J., J. A. Smith, and F. G. Hall. 1988. Characterising Forest Ecosystem Dynamics through Modeling and Remote Sensing Observations. Paper read at IGARSS Symposium, Edinburgh, Scotland.

Sampson R. N., Adams D. L., Hamilton S. S., Mealey S. P., Steele R., Van de Graaff D. 1994. Assessing Forest Ecosystem Health in the Inland West. Haworth Press, New York.

Sloan, J. 2010. The Use of the Civil Air Patrol ARCHER Hyperspectral Imagery for Forest Health and Multi-Stage Conifer Mortality. In AAG 2010 Annual Meeting, Washington D.C.

Taylor, A. H. and C. N. Skinner. 2003. Spatial Patterns and Controls on Historical Fire Regimes and Forest Structure in the Klamath Mountains. *Ecological Applications.* 13: 704–719

Van Aardt, J. A. N. and R. H. Wynne. 2007. Examining Pine Spectral Separability Using Hyperspectral Data from an Airborne Sensor: An Extension of Field-Based Results. *International Journal of Remote Sensing* 28 (1-2):431-436.

Van Aardt, J. A. N. 2000. Spectral Separability among Six Southern Tree Species. University Libraries, Virginia Polytechnic Institute and State University. Blacksburg, Va.

Whitworth, J. and K. Reed. 2007. Playing with Fire - Reintroducing Fire to Colorado Forests. In AAG Great Plains - Rocky Mountain Division 2007 Annual Meeting, Denver, CO.

Wightman, C. S. and S. S. Germaine. 2006. Forest Stand Characteristics Altered by Restoration Affect Western Bluebird Habitat Quality. *Restoration Ecology* 14 (4):653-661.

Yang, C., J.H. Everitt, R.S. Fletcher, R.R. Jensen and P.W. Mausel. 2009. Evaluating AISA Hyperspectral Imagery for Mapping Black Mangrove Along the South Texas Gulf Coast. *Photogrammetric Engineering and Remote Sensing*. 75: 425-435\

Zare, A. 2008. Hyperspectral Endmember Detection and Band Selection using Bayesian Methods. Ph.D. Dissertation, University of Florida.